ELSEVIER

Thermochimica Acta 288 (1996) 203–219

thermochimica acta

A kinetic and mechanistic study of the thermal decomposition of calcium nitrate

Clodagh Ettarh [a,b], Andrew K. Galwey [a,*]

[a] *School of Chemistry, The Queen's University of Belfast, Belfast BT9 5AG, UK*
[b] *Questor centre, The Queen's University, Belfast BT9 5AG, UK*

Received 18 January 1996; accepted 17 June 1996

Abstract

Anhydrous calcium nitrate melts at 836 ± 2 K and subsequent decomposition occurs in the liquid phase. The temperature of NO_3^- anion breakdown under dynamic rising temperature conditions increases with the heating rate, being 949 K at 10 K min^{-1}. Kinetic studies of this pyrolysis are reported from observations obtained by two complementary isothermal techniques. From measurements of gaseous product evolution in an evacuated constant volume apparatus between 773 and 820 K (this reaction is approximately summarised as $Ca(NO_3)_2 \rightarrow CaO + 1(1/2)NO_2 + O_2 + (1/4)N_2$) it was shown that data were well expressed by the Avrami-Erofe'ev equation ($n = 2$) and the activation energy (E) was 229 ± 10 kJ mol^{-1} between $0{\cdot}10 <$ fractional reaction, α, < 0.85. An alternative titration technique, based on the evolution of products ($NO + NO_2$) between 818 and 848 K, identified a different pattern of kinetic behaviour. Two linear regions of the α-time curves were found, the first between $0.3 < \alpha < 0.6$ ($E = 217 \pm 9$ kJ mol^{-1}) and the second, relatively more rapid, between $0.7 < \alpha < 0.9$ and $E = 298$ kJ mol^{-1}. Mechanistic interpretations lead us to conclude that anion breakdown occurs in two overlapping and interacting steps: nitrate → nitrite → oxide.

Some environmental implications of these observations are discussed that may be of value in the development of technology for use in pollution abatement by removal of NO_x from industrial flue gases.

Keywords: Acid rain; Calcium nitrate; Decomposition kinetics; Melt reaction

1. Introduction

Emissions from power stations released into the atmosphere contain significant amounts of nitrogen oxides (NO_x) that are recognised as precursors to acid rain [1,2].

* Corresponding author.

PII: S0040-6031(96)03052-3

At present flue gases are not specifically treated to remove or to minimise this source of pollution. Greater effort, backed by extensive research [3], has been directed towards decreasing the relatively larger releases of sulphur oxides (SO_x) that are generated in large scale coal burning plants [2,4]. Sulphur is a constituent of this fuel and, unless preventative measures are taken, a high proportion is converted directly to oxides that are dispersed in the air. A proportion of the NO_x, that is also produced during the generation of electricity from coal, may similarily derive from the fuel but additional NO_x may be formed during high-temperature combustion [5,6]. Control of air oxidation, the reaction of N_2 with O_2, can be achieved by changes in flame structure [5–7] and this approach is used to minimise NO_x releases. Consequently the treatment of flue gases has most usually been concerned with desulphurisation [8–15], which can be exploited as a resource yielding products of some commercial value, such as $CaSO_4$ or H_2SO_4.

Significant removal of sulphur oxides during low temperature combustion of flue gases cooled below 1300 K can be achieved using calcite. Under oxidising conditions SO_x is converted to the relatively stable $CaSO_4$, most usually produced through the *sulphation reaction* [8–12,16]:

$$CaCO_3 + SO_2 + \frac{1}{2}O_2 \rightarrow CaSO_4 + CO_2 \quad (1)$$

Above about 1500 K there is thermal decomposition of $CaSO_4$ [5,17] or reduction by CO at somewhat lower temperatures [18]. Sulphur removal by calcite is most effective in the relatively low temperature chain grate furnaces or by the injection of finely powdered $CaCo_3$ into the partially cooled gaseous products of higher temperature oxidation. An important characteristic of the sulphation reaction is that $CaSO_4$ product forms a comprehensive and coherent barrier between the reactants [3,16, 19–21]. This restricts the extent of reaction (1) and may effectively prevent complete conversion of all the $CaCO_3$ to $CaSO_4$, particle centres remain unreacted. The method is wasteful of a resource and crushing the calcite sufficiently finely to enable reaction to proceed to completion may be difficult to achieve [16,22]. The alternative use of the more reactive $Ca(OH)_2$ is more expensive.

An aspect of the use of $CaCO_3$ in flue gas desulphurisation that does not appear to have been examined in detail is the possibility of participation by reactions involving NO_x, perhaps including the intervention of $Ca(NO_3)_2$. This is of some theoretical interest and may also have practical importance. It is known that calcium nitrate is formed by the reactions of nitrogen oxides with $CaCO_3$ and with CaO [23–25], a brief investigative study of the reactions of NO_2 with $CaCO_3$ is reported here. Accordingly, it was considered to be of interest to examine the possibility that $Ca(NO_3)_2$ may participate in the chemical treatments used to remove the precursors of acid rain from flue gases for the following reasons. $Ca(NO_3)_2$ melts before decomposition [21,26,27]. This involvement of a liquid phase could be beneficial in increasing both rates and extents of desulphurisation by diminishing the effectiveness of the $CaSO_4$ barrier layer in opposing the sulphation reaction (1) [16]. Secondly, nitrite or nitrate formed by reaction of NO_x with $CaCO_3$ may contribute to sulphation by oxidising SO_2 and/or $SO_3^=$ ($CaSO_3$) to $CaSO_4$ [28]. These reactions could contribute to flue gas denitrification by diminishing NO_x releases.

For these reasons it was considered to be timely and appropriate to undertake a kinetic and mechanistic study of the thermal decomposition of $Ca(NO_3)_2$. Previous studies of this reaction have been reported by Doumeng [29] and Warrington [30]. We have already investigated the catalytic properties of a number of oxides in promoting $Ca(NO_3)_2$ decomposition [31]. Transition metal oxides were found to be the most active and we concluded that in most of these reactions anion breakdown occurred in a melt.

Knowledge of the reactivity of $Ca(NO_3)_2$ as the most stable, and, indeed, most probable participant in these reactions, is regarded as providing essential background information that can be used in characterising a possible role of NO_x in flue gas treatments with calcite. The present work was completed for this purpose and the relevance of the results is discussed in the context of pollution abatement. Subsequent investigations, currently being prepared for publication [28], are concerned with the ability of $Ca(NO_3)_2$ to oxidise $CaSO_3$ or SO_2 to $CaSO_4$. This is an alternative to the sulphation reaction and a possible route to the diminution of emissions that cause acid rain.

PART 1: DECOMPOSITION REACTIONS OF $Ca(NO_3)\cdot xH_2O$

2. Experimental

2.1. Apparatus

Rising temperature experiments were completed in a Perkin-Elmer DSC 7 and all calculations used the software supplied by the manufacturer. Reactant samples were contained in gold pans covered with loosely fitting lids.

Isothermal rate measurements were made in a conventional glass vacuum apparatus, evacuated < 0.1 Nm^{-2} before each kinetic experiment. Pressures of evolved product gases were determined using an MKS 222B absolute pressure gauge working in the range 0–1500 Nm^{-2} and read with an accuracy ± 0.1 Nm^{-2}. The apparatus and procedure have been described in detail by Carr and Galwey [32]. (Pressure, time, temperature) data were collected and recorded for later analyses and testing of kinetic fit. No refrigerant trap was used during the present investigations that were concerned with total evolution of all gaseous products.

A complementary isothermal study of the evolution of acid gases (NO and NO_2) from $Ca(NO_3)_2$ decomposition was completed by a titration method previously described [33]. A known weight (ca. 0.25g) of reactant was held at constant temperature ($\pm$ 1K) in a tube furnace through which a flow of argon (160 cm^3 min^{-1}) was maintained. The gases were bubbled through a stirred beaker containing water, a small amount of H_2O_2 (0.5 cm^3 of 10% H_2O_2, to aid the initial formation of HNO_3[34]), indicator and a glass electrode to monitor pH. By titrating the acid formed through addition of standard 0.25M NaOH at recorded times the kinetics of (NO and NO_2) formation (yielding HNO_2 and HNO_3) could be measured.

Reactant $Ca(NO_3)_2\cdot xH_2O$ was GPR Anhydrous as supplied by BDH. The magnitude of x was less than 1.0 and resulted from water uptake during minimum exposures of this deliquescent salt to the atmosphere.

3. Results and discussion

3.1. Rising temperature experiments

A typical DSC response trace obtained on heating $Ca(NO_3)_2$ (dehydrated, but retaining a small amount of water) from 323 to 1000 K at 10 K min^{-1} in a flowing nitrogen atmosphere is shown in Fig. 1. The first irregular response, *ca* 420–460 K, is identified as volatilisation of the residual retained water and was absent when more effectively dehydrated salt was used. The first sharp endotherm is identified as melting. The subsequent responses, the several subsidiary peaks followed by a dominant maximum seen in Fig. 1, are due to salt decomposition. These were appreciably irreproducible between successive, but apparently identical, experiments. This is evidence that more than a single rate process is involved. More than sixty experiments were completed to establish reliably the effects on reaction of changes of heating rate, disposition of the sample within the reaction chamber and reaction zone atmosphere (N_2 or air) on DSC response patterns that were invariably endothermic. The results are summarised as follows.

3.2. $Ca(NO_3)_2$ melting

The mean measured melting point of calcium nitrate was 836 ± 2 K. This endotherm maximum varied only slightly with heating rate: 836.7 ± 0.7 K at 5 K min^{-1} (regarded as the most reliable value), 836.6 ± 3.5 K at 10 K min^{-1} and 833 ± 6 K at 20 K min^{-1}. Melting was only partially reversible. For example, the melting point recorded for a particular sample heated at 10 K min^{-1} was 840 K but, after immediate cooling from

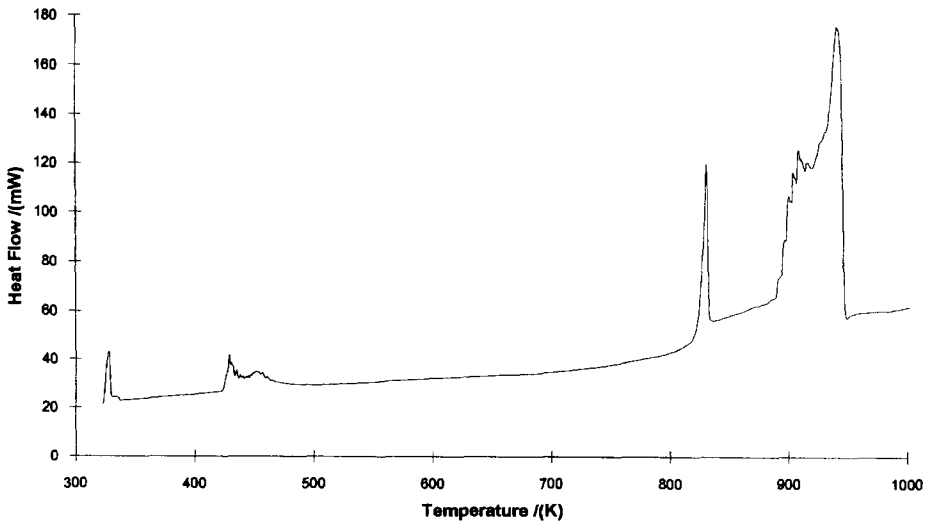

Fig. 1. A typical DSC response trace for $Ca(NO_3)_2 \cdot xH_2O$ heated at 10 K min^{-1}.

the maximum temperature reached 843 K, solidification occurred at the significantly reduced temperature, 813 K. While supercooling could contribute to the difference, it is considered more probable that some salt decomposition yielded $Ca(NO_2)_2$ that depressed the recrystallisation temperature. This explains why the enthalpy of fusion value measured here, $27 \pm 3\,kJ\,mol^{-1}$ for heating at $20\,K\,min^{-1}$, is appreciably larger than the literature value $23.4\,kJ\,mol^{-1}$ [35]. The apparent magnitude of the enthalpy of fusion increased with diminution in the heating rate (36 and $40\,kJ\,mol^{-1}$ measured for heating at 10 and $5\,K\,min^{-1}$ respectively) and is ascribed to the longer heating times (accompanied by more reaction) required to complete sample melting.

Alternative dispositions of the salt crystallites within the gold pan as a thin layer or as an aggregate caused no change in the measured melting point. Similarly there was no change in the melting temperature for samples heated in N_2 or in air. The melting point reported here compares well with other values reported in the literature [21,30,36].

3.3. $Ca(NO_3)_2$ decomposition

The mean temperatures of the dominant endotherm maximum identified as decomposition (Fig. 1) increased systematically with rise in the heating rate from 932 K at $5\,K\,min^{-1}$ to 949 K at $10\,K\,min^{-1}$ and 952 K at $20\,K\,min^{-1}$. Uncertainties were relatively large, ± 15 K, due to variations in the response peak shape between successive nominally identical experiments. However, from careful comparison of all our data, we detected no systematic changes in the pattern of anion breakdown with: (i) the presence of small amounts of water in the original reactant (which were, however, released well below the temperature of salt decomposition), (ii) reactant mass (5 to 12 mg) or salt disposition within the containing pan, (iii) pregrinding of the original reactant solid, and (iv) decomposition in an air or N_2 atmosphere. (Bond and Jacobs[37] have similarly shown that the rates of $NaNO_3$ decomposition are identical in air and argon.) These results are consistent with the conclusion that anion breakdown proceeds through an activated reaction in the molten salt.

Apparent values of the decomposition enthalpy increased appreciably with the heating rate from $315 \pm 20\,kJ\,mol^{-1}$ at $5\,K\,min^{-1}$ to $334 \pm 50\,kJ\,mol^{-1}$ at $10\,K\,min^{-1}$ and $401 \pm 70\,kJ\,mol^{-1}$ at $20\,K\,min^{-1}$. As already stated, some decomposition accompanies melting, introducing systematic errors into these values. The trend is also consistent with the possibility that more than a single process contributes to the overall reaction. These magnitudes are consistent with the formation of a high proportion of NO_2 in the volatile reaction products, suggesting that stoichiometry may be approximately represented by the following equations:

$$Ca(NO_3)_2 \rightarrow CaO + 2NO + 1\tfrac{1}{2}O_2$$

$$Ca(NO_3)_2 \rightarrow CaO + NO_2 + NO + O_2$$

$$Ca(NO_3)_2 \leftrightarrow CaO + 2NO_2 + \tfrac{1}{2}O_2$$

for which the reaction enthalpies calculated from the thermochemical data are 369, 426 and $482\,kJ\,mol^{-1}$ respectively (values from 'Handbook of Chemistry' sources).

3.4. Isothermal kinetic studies of $Ca(NO_3)_2$ decomposition

(a) Constant volume apparatus

Extents of reaction were measured from the total pressure of all gases evolved in the constant volume evacuated system at known times, no refrigerant trap was used. Kinetic studies were completed across the temperature interval 773 to 820 K.

Representative fractional reaction (α)-time plots are shown in Fig 2. The main rate process was preceeded by the evolution of a small amount of gas (completed at α = approx. 0.05) that probably represented the onset of decomposition accompanied by melting. Thereafter the reaction accelerated briefly (when $\alpha < 0.2$) reaching a rate that remained constant between $0.3 < 0.7$: this zero order behaviour was the dominant kinetic characteristic of this reaction. Thereafter the rate decelerated to completion ($\alpha = 1.00$).

The most satisfactory kinetic fit to these sigmoid shaped curves was given by the Avrami-Erofe'ev equation [38,39], $n = 2$, between $0.10 < \alpha < 0.85$, plots for the data in Fig. 2 are given in Fig. 3. During the final stages ($\alpha > 0.85$) the process was less deceleratory than the requirements of this equation leading to a more rapid completion and an increase in the slope of the plots in Fig. 3. The significance of this kinetic analysis will be discussed further below but is here presented as the rate equation that most satisfactorily represents the data. From these rate constants the calculated activation energy was $229 \pm 10\,kJ\,mol^{-1}$ (773 to 820 K).

Weight losses on completion of salt decomposition were in accordance with the expectation that CaO was the only residual product. Partial analyses of the product gases were achieved by the use of cold traps and the known volume of the apparatus.

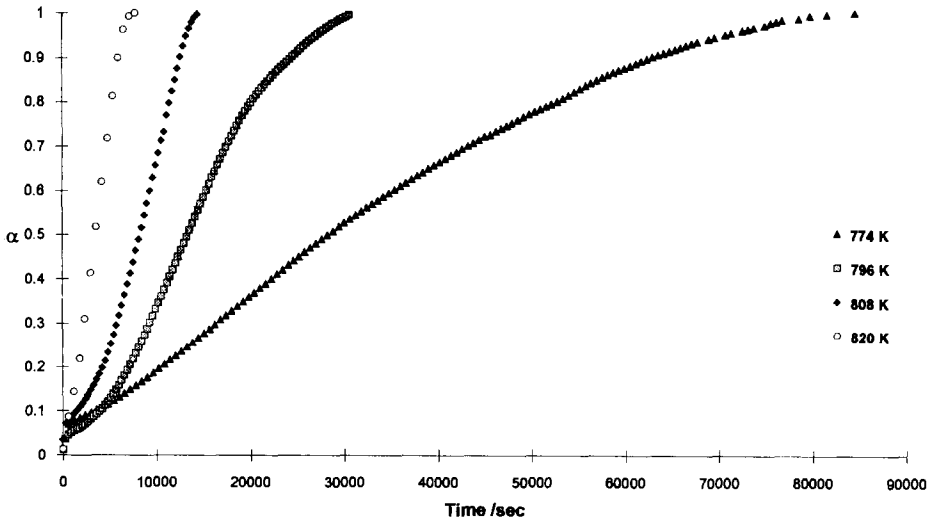

Fig. 2. Representative α-time plots for the isothermal decomposition of $Ca(NO_3)_2 \cdot xH_2O$ in vacuum at selected temperatures from response measurements of gas evolved in evacuated apparatus.

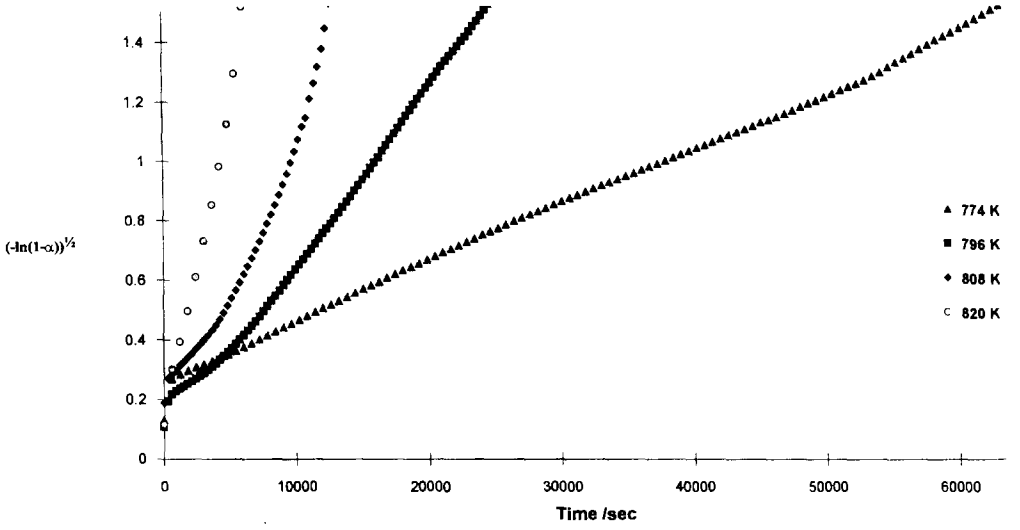

Fig. 3. Plots of $(-\ln(1-\alpha))^{1/2}$ versus time for the decomposition of $Ca(NO_3)_2 \cdot xH_2O$ in vacuum, same experiments as in Fig. 2.

(At 78 K only N_2 and O_2 are volatile and NO exerts a pressure of 30 Nm^{-2}. At 178 K, N_2, O_2, N_2O and NO are volatile. The reaction $2NO + O_2 \rightarrow 2NO_2$ is expected to proceed to completion in the apparatus at ambient temperature.) Partial analyses of the products of all completed decompositions showed that O_2 and NO_2 were the dominant gaseous products and that under these conditions the reaction (773 to 820 K) was most satisfactorily represented by the equation:

$$Ca(NO_3)_2 \rightarrow CaO + 1\frac{1}{2}NO_2 + O_2 + \frac{1}{4}N_2$$

(b) Titration apparatus

During these experiments gaseous products were swept continually from the isothermal ($\pm$ 1 K) reaction zone in an inert (argon) atmosphere and dissolved in water. Extents of reaction (α) at known times were measured by titration of the amounts of standard alkali (0.25M NaOH) required to neutralise the acid formed by reaction of the NO and NO_2 evolved during the $Ca(NO_3)_2$ decomposition. The following reactions occur in the presence of alkali:

$$2NO_2 + 2NaOH \rightarrow NaNO_2 + NaNO_3 + H_2O$$

$$NO + NO_2 + 2NaOH \rightarrow 2NaNO_2 + H_2O$$

Fractional decomposition (α) values were calculated from the total addition of alkali required to neutralise the acid after time t divided by the total volume required on final completion of salt decomposition. Representative α-time plots are shown in Fig. 4.

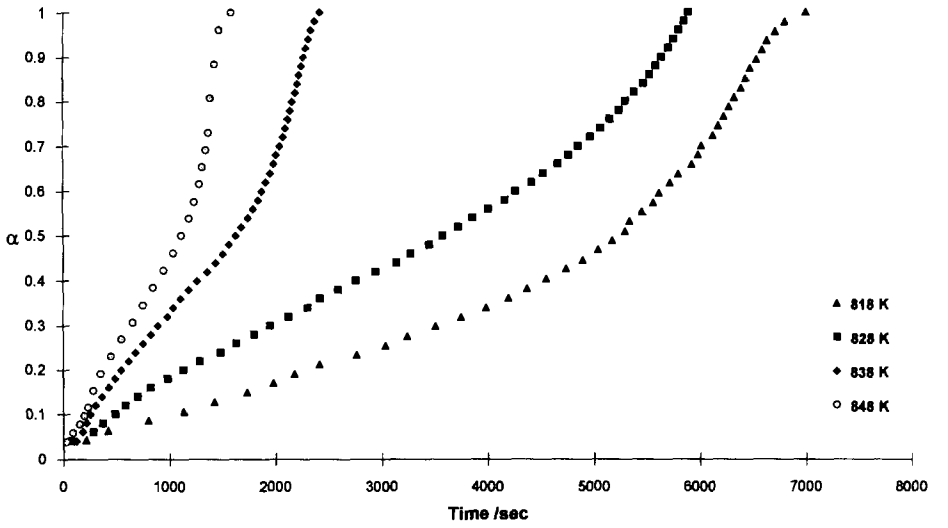

Fig. 4. Representative α-time plots for the isothermal decomposition of $Ca(NO_3)_2 \cdot xH_2O$ at selected temperatures from titration apparatus.

Three stages in the rate process can be distinguished. There is a rapid initial small gas evolution (α = approx. 0.05), identified as decomposition accompanying melting. This was followed by an approximately zero order reaction between $0.1 < \alpha < 0.5$. Reaction then accelerated to give a second brief constant reaction rate between ($0.7 < \alpha < 0.9$) before the final decleration to completion of decomposition.

Quantitative kinetic analyses of these curves by a single rate expression is not possible. The later acceleratory stage is not characteristic of any simple homogeneous reaction model or indeed of a heterogeneous kinetic expression [39]. Critical examination of the non-linear Avrami–Erofe'ev plots (prepared to enable these data to be compared with the vacuum apparatus results) showed that α-time curve shapes varied with reaction temperature. This was confirmed by the calculation of apparent activation energy values (818 to 848 K) for the two linear regions in Fig. 4: $217 \pm 9\ kJ\ mol^{-1}$ between $0.3 < \alpha < 0.6$ and $298 \pm 8\ kJ\ mol^{-1}$ for the later stages, $0.7 < \alpha < 0.9$.

Total yields of acid gases on completed $Ca(NO_3)_2$ decomposition corresponded to 1.0 mole (NO and NO_2)/mole $Ca(NO_3)_2$. These yields, from reaction under dynamic conditions, are less than those found from reactions under accumulatory conditions.

3.5. *Electron microscopic observations*

The scanning electron microscope was used to obtain information concerning textural changes during $Ca(NO_3)_2$ decomposition. These observations were concerned with reactant that had been cooled after the onset of reaction, $\alpha = 0.10$, at approx. 840 K and the final residual product ($\alpha = 1.00$).

(a) Salt decomposition to $\alpha = 0.10$

Representative textures of partly decomposed reactant are shown in Figs. 5, 6 and 7. The wrinkled surfaces, the rounded textures and the absence of sharp edged features are consistent with comprehensive reactant melting. The more complex features are probably bubble formation that occurred during product gas evolution.

Fig. 5. Wrinkled area adjacent to smooth surface in partially decomposed $Ca(NO_3)_2 \cdot xH_2O$ ($\alpha = 0.10$).

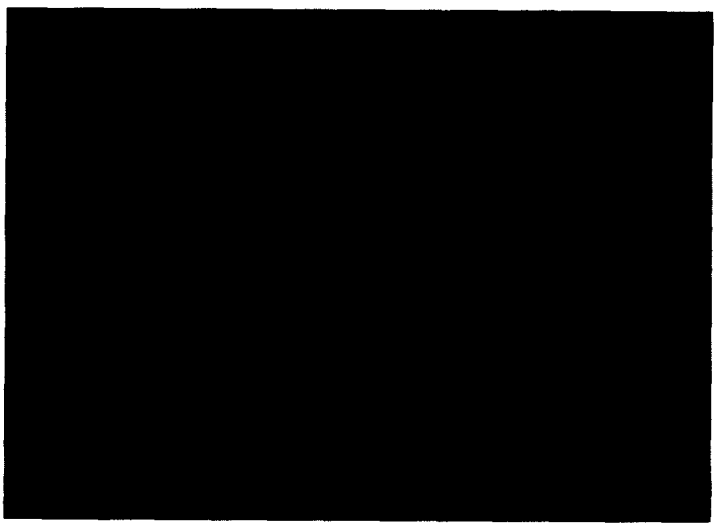

Fig. 6. Partially decomposed $Ca(NO_3)_2 \cdot xH_2O$ indicating channels of melt with unreacted salt beneath. ($\alpha = 0.10$).

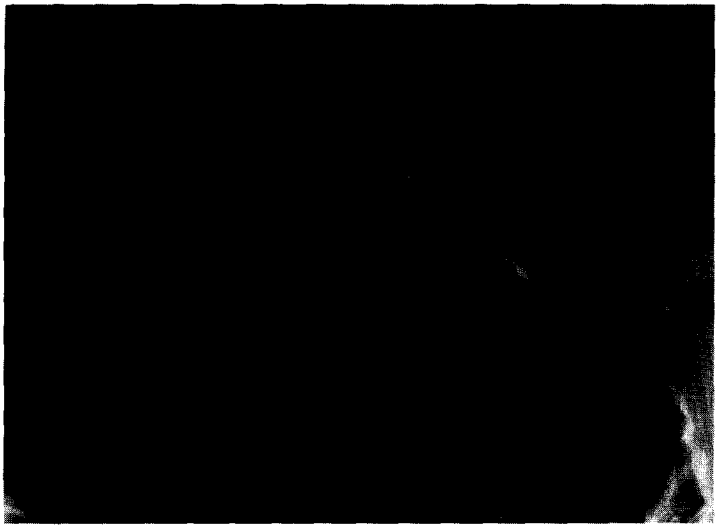

Fig. 7. Froth appearance indicating gas evolution. ($\alpha = 0.10$).

(b) Decomposed salt ($\alpha = 1.00$)

The residual product, Fig. 8, was composed of particles bounded by flat faces with some defects. This is identified as crystalline CaO formed as the final product of anion breakdown in the fluid reactant.

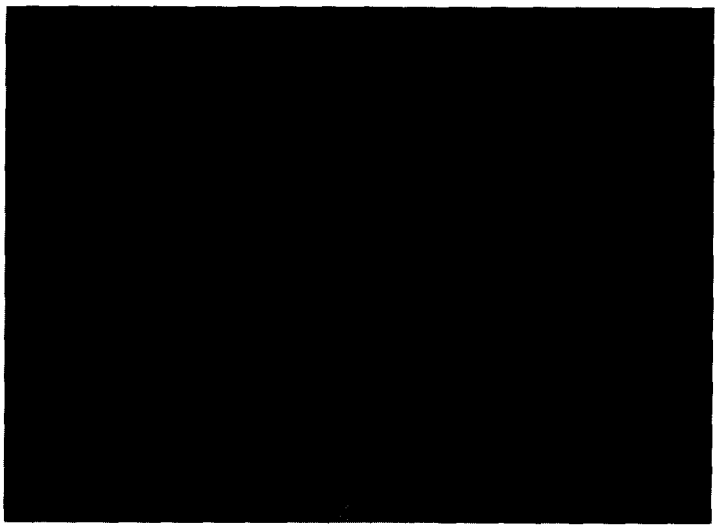

Fig. 8. Completely decomposed $Ca(NO_3)_2 \cdot xH_2O$. ($\alpha = 1.00$).

4. Conclusions

4.1. Melting

There is no evidence that $Ca(NO_3)_2$ decomposes in the solid state, but in the dynamic heating experiments melting at 836 ± 2 K is accompanied by a small amount (ca. 5%) of anion breakdown.

4.2. Stoichiometry

Doumeng [29] has discussed the reactions which may be expected to contribute to and participate in anion breakdown on heating calcium nitrate. These include the following:

$$Ca(NO_3)_2 \rightarrow Ca(NO_2)_2 + O_2 \quad (2)$$

$$Ca(NO_2)_2 \rightarrow CaO + 2NO + \frac{1}{2}O_2 \quad (3)$$

$$Ca(NO_2)_2 \rightarrow CaO + NO + NO_2 \quad (4)$$

$$Ca(NO_2)_2 + 2NO_2 \leftrightarrow Ca(NO_3)_2 + 2NO \quad (5)$$

$$Ca(NO_2)_2 + 2NO \leftrightarrow Ca(NO_3)_2 + N_2 \quad (6)$$

Nitrite formation is the most probable first step and this may occur during reactant melting. Differences in the temperature coefficients for these several processes explain the variations in shapes of α-time curves and product yields with reaction temperature. The overall reaction stoichiometry from the present observations of the yields of condensable and permanent gas products may be approximately expressed as:

$$Ca(NO_3)_2 \rightarrow CaO + \frac{1}{4}N_2 + O_2 + 1\frac{1}{2}NO_2$$

though when product gases were swept rapidly from the reaction zone the observed yields of nitrogen oxides were relatively diminished (1.0 mole $(NO + NO_2)$).

4.3. Kinetics

Because the formation of the several reaction products result from the contributions from more than a single rate process, it cannot be expected that the overall kinetic behaviour will be represented by a simple rate equation. It has been observed here that the shapes of the α-time curves vary with temperature. Mindful of these variations we can make only a qualitative analysis of the rate characteristics.

Rate studies based on accumulatory gas evolution experiments between 773 to 820 K (below the normal melting point, 836 K) gave sigmoid shaped α-time curves. These represent the cumulative outcome of the evolution of oxygen from reaction (2)

and nitrogen oxides (mainly NO_2) from nitrite breakdown, reactions (3–6) together with $2NO + O_2 \rightarrow 2NO_2$. It is expected that nitrite formation from reaction (2), will result in progressive melting of the reactant; $Ca(NO_2)_2$ melts [30] at 654 K. The subsequent nitrite decomposition will result in approximately zero order overall behaviour. A somewhat similar kinetic behaviour pattern has been reported for the decomposition of lithium potassium tartrate [38] (for which the activation energy value was also 220 kJ mol^{-1}). Two mechanistic explanations (or combinations of these) are consistent with the sigmoid shaped curve including a constant rate during the median range: (i) progressive melting accompanied by decomposition in the liquid (Avrami–Erofe'ev equation) or (ii) decomposition of a decreasing amount of nitrate together with the breakdown of an increasing amount of nitrite.

The initial rate of ($NO + NO_2$) formation, measured by the titration method, 818 to 848 K, was approximately zero order and is believed to be the same process as the constant rate reaction identified (773 to 820 K) under accumulatory conditions. Levels of reactivity and activation energy values are similar but direct comparisons of rate constants are not possible here because α values are based on yields of more than a single product generated by two or more reactions.

The significant differences in kinetic behaviour characteristic of the titration experiments are ascribed to the relative increase in rates of formation of (NO and NO_2) during the latter stages together with the greater activation energy for the higher α range. No kinetic discontinuity or non-linearity of the Arrhenius plot attributable to melting was discerned and it was concluded that reaction occurred in the liquid phase. (The sigmoid shaped curves in Fig. 2 may, however, arise through melting as a contributory controlling factor, influencing reaction rate.)

The relative increase in rates of ($NO + NO_2$) formation later in the reaction (Fig. 4) may be ascribed to nitrite breakdown which follows the nitrate reaction (2) that yields oxygen. Accordingly the overall pattern of anion breakdown can be ascribed to the two dominant controlling reactions:

$$Ca(NO_3)_2 \rightarrow Ca(NO_2)_2 + O_2 \quad (2)$$

$$Ca(NO_2)_2 \rightarrow CaO + NO_2 + NO \quad (4)$$

Perhaps the latter is somewhat more rapid than the former, nitrites are generally less stable than the nitrates. Other concurrent or subsequent reactions undoubtably participate.

The activation energy for reaction (2), *ca.* 220 kJ mol^{-1}, is estimated to be only slightly greater than the calculated difference between heats of formation of $Ca(NO_3)_2$ and $Ca(NO_2)_2$. Thus the greater proportion of the activation energy requirement is due to the endothermic character of the reaction. A similar conclusion was reached for $Ca(NO_2)_2$ decomposition. Thus the highly endothermic character of the overall decomposition of calcium nitrate (values of 369, 426 and 482 kJ mol^{-1}, depending on products formed as mentioned above) requires a two step decomposition, each with a relatively large activation energy. The present observations are satisfactorily explained by stepwise breakdown of the anion $NO_3^-(-\frac{1}{2}O_2) \rightarrow NO_2^-(-(\frac{1}{2}NO_2 - \frac{1}{2}NO) \rightarrow \frac{1}{2}O^=$ [37].

PART 2. REACTIONS OF NO_2 WITH $CaCO_3$

Previous studies [23–25] have shown that both NO and NO_2 react with calcite to form $Ca(NO_3)_2$. To investigate the possibility that these reactions may occur under the conditions of flue-gas treatments, we undertook the following preliminary experiments. Samples of $CaCO_3$ in the form of a fine powder (approximately cube-shaped crystallites, edges 5–10 μm [16]) or freshly cleaved (100) faces of larger calcite crystals (edges approximately 5 mm) were exposed to a flowing NO_2 (10 to 25%) and air mixtures for various times, 1 to 20 min at 570, 670 or 770 K. The reacted solid products were examined by thermal analysis (DSC) and by electron microscopy.

Our observations confirmed positively that $Ca(NO_3)_2$ was produced in these reactions. Weight increases for the powdered samples tended to be irreproducible, probably due to variations in diffusive access of the gaseous reactant to particles within the powder aggregate. A 5–10 min reaction at 770 K converted, on average, 10–15% calcite to $Ca(NO_3)_2$. Nitrate yields from reactions at 570 and 670 K were somewhat less, 5–10%.

5. DSC Traces

Representative DSC response traces for the product of the NO_2 and $CaCO_3$ reactions at 770 (B) and 570 (C) K are compared with a trace for pure $Ca(NO_3)_2$ in Fig. 9. The NO_2 and $CaCO_3$ products show an initial endotherm at 812 K, followed by a subsidiary maximum before the large endotherm, maximum 905 K, completed by 912 K. These temperatures are below those characteristic of the pure salt, which melts at 836 K, the decomposition endotherm maximum is at 949 K, completed by 965 K.

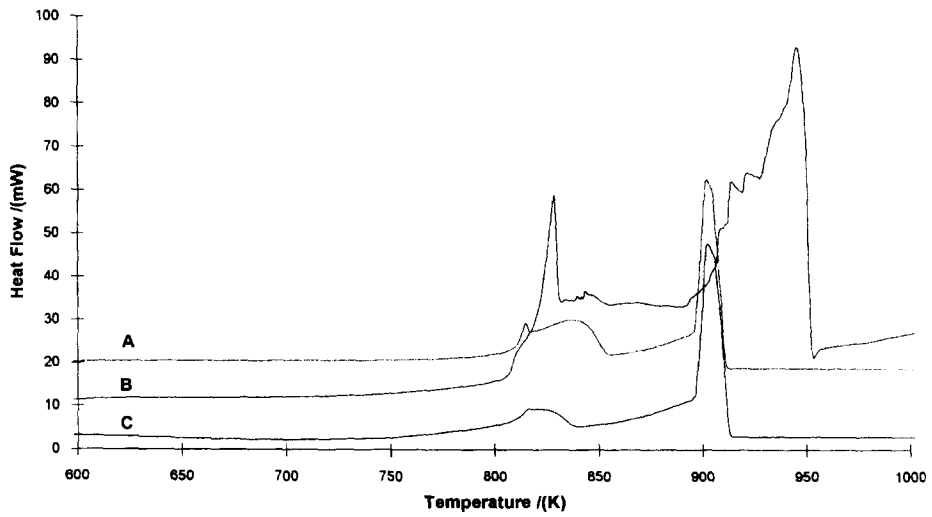

Fig. 9. Typical DSC traces for: (A) $Ca(NO_3)_2 \cdot xH_2O$ (B) $CaCO_3$ reacted with NO_2 at 770 K (C) $CaCO_3$ reacted with NO_2 at 570 K.

Our observations are explained by the formation of $Ca(NO_3)_2$ but the melting and decomposition temperatures are evidently diminished somewhat by the $CaCO_3$ with which it is expected to interact. There was no evidence, from the DSC traces, of $Ca(NO_2)_2$ formation, this compound is reported [30] to melt at 654 K, though other values (650–655 K) have been given [35,40,41]. The absence of this product is consistent with the evidence [29,30] that $Ca(NO_2)_2$ is oxidised by NO_2 (reaction 5).

6. Electron microscopic studies

Figure 10 shows a typical texture of $CaCO_3$ powder particles after reaction in a NO_2: air (1 : 3) mixture for 3 min at 770 K. Crystallite aggregates have been formed by sintering and sharp corners have become rounded apparently by superficial liquifaction.

The typical appearance of cleaved (100) calcite surfaces after reaction for 3 min at 770 K in NO_2 : air (1 :4) is shown in Figs. 11 and 12. The textures are attributable to the formation of a viscous superficial liquid in which there has been bubble formation, identified as the release of CO_2 accompanying $Ca(NO_3)_2$ formation. The torn surfaces of burst bubbles are seen in Fig. 11 and wrinkling due to bubble contraction and collapse during cooling are seen in Fig. 12. The line feature across Fig. 12 is characteristic of surface tension effects following melting at the step edges on $CaCO_3$ that appear after cleavage.

7. Comment

The above observations are completely satisfactorily explained by the formation of a superficial $Ca(NO_3)_2$ layer following the reaction of $CaCO_3$ and NO_2. It appears that the reaction occurs in a liquid phase, that presumably incorporates some $CaCO_3$,

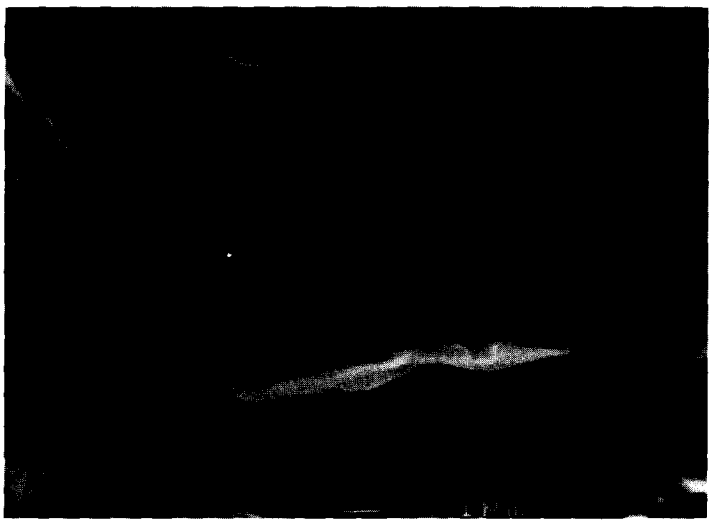

Fig. 10. Electron micrograph of $CaCO_3$ reacted with NO_2 and air mixture (1 : 3) at 770 K.

Fig. 11. Micrograph indicating melt bubbles from the reaction of $CaCO_3$ with NO_2 and air mixture (1 : 4) for 3 min at 770 K.

Fig. 12. Nucleation sites on $CaCO_3$ crystal reacted with NO_2 and air mixture (1 : 4) for 3 min at 770 K.

together with the possible intervention of $Ca(NO_2)_2$, though we obtained no evidence of the accumulation of appreciable quantities of this intermediate. Bubble evolution is ascribed to CO_2 release during the reaction. These observations support the conclusion that significant quantities of $Ca(NO_3)_2$ are formed during reactions of nitrogen oxides with calcite between approximately 600–800 K. These may be similar to flue gas treatment conditions.

8. Conclusions

8.1. Denitrification and desulphurisation reactions

One objective of the present study was to investigate the chemical characteristics of $Ca(NO_3)_2$ to establish whether the properties and reactivities of this compound offer any promise for use in the removal of the NO_x precursors to acid rain in flue gases produced in coal combustion. It must be concluded, however, that the reactions reported here offer little direct use in denitrification because $Ca(NO_3)_2$ breakdown predominantly yields NO_2. The range of oxides investigated to promote this reaction [31] gave little evidence of any improvement. It is, however, expected that significant amounts of $Ca(NO_3)_2$ would not be formed at the temperatures [16] of the sulphation reaction (1). A further possibility, not investigated here, is that if $Ca(NO_3)_2$ decomposition proceeded in the presence of ammonia the intervention of the unstable NH_4NO_2 might yield $N_2 + H_2O$.

Consideration of the present results indicated a number of lines for possible future development, most notably our preliminary observation [28] that $Ca(NO_3)_2$ reacts at relatively low temperatures with $CaSO_3$ and with SO_2 to give $CaSO_4$. A study of these reactions will be the subject of a future paper. An interesting feature of the reaction is the participation of a liquid phase that diminishes the effectiveness of the product barrier layer of $CaSO_4$ in opposing the sulphation reaction.

References

[1] N.J. Bunce, Environmental chemistry, Wuerz Publishing, Winnipeg, 1990.
[2] J.E. Ferguson, Inorganic chemistry and the earth, Pergamon, Oxford, 1982.
[3] D.C. Anderson and A.K. Galwey, Proc. R. Soc. London, Ser. A, 452 (1996) 585, 603.
[4] N.H. Ulerich, E.P. O'Neill and D.L. Keairns, Thermochim. Acta, 26, (1978) 269.
[5] M.J. Cooke and R.J. Pragnell. Energy and the Environment, Symp. 1990, Spec. Publication R. Soc. Chem., London, 1990, p. 224.
[6] J.H. Howarth and T.R. Bott, NATO ASI Series, E145 (1988) 679.
[7] J.P. Smart, K.J. Knill, B.M. Visser and R. Webber, Proc. 22nd Internat. Symp. Combustion (Combustion Institute) 1989, p. 1117.
[8] D.C. Fee, N.I. Wilson, K.M. Myles and I. Johnson, Chem. Eng. Sci., 38 (1983) 1917.
[9] J.S. Dennis and R.B. Fieldes, Chem. Eng. Res. Des., 64 (1986) 279.
[10] A.O. Denloye, L.L. Gasner and F.R. Adamchak, Thermochim. Acta, 75 (1984) 9.
[11] S. Osuwan, K. Bunyakiat and D. Theerapabpisit, J. Sci. Soc. Thailand, 15 (1989) 17.
[12] G.A. Simons, T.E. Parker and J.R. Morency, Combus. Flame, 74 (1988) 107.
[13] W.D. Halstead, Research (CEGB, London), Sept. 1988 p. 3.
[14] P. Fuchs, B. Roth, U. Schwing, H. Angele and J. Gottstein, Radiat. Phys. Chem., 31 (1988) 45.
[15] S. Jordan, Radiat. Phys. Chem., 31 (1988) 21.
[16] D.C. Anderson, P. Anderson and A.K. Galwey, Fuel, 75 (1995) 1018, 1024, 1031.
[17] F. Hanic, L. Galikova, J. Havlica, I. Kapralik and V. Ambruz, Brit. Ceram. Trans. J., 84 (1985) 22.
[18] S. Ghardashkhani and O. Lindqvist, Thermochim. Acta, 195 (1992) 113.
[19] M.H. Erten, Coal Sci. Technol., 9 (1985) 451.
[20] R.K. Chan, K.S. Murthi and D. Harrison, Can. J. Chem., 48 (1970) 2979.
[21] B.O. Field and C.J. Hardy, Quart. Rev., 18 (1964) 361.
[22] N.A. Burdett, J.R.P. Cooper, S. Dearnley, W.S. Kyte and M.F. Tunnicliffe, J. Inst. Energ., 58 (1985) 64.

[23] G. Gut, M.J. Abd-Ellatif and A. Guyer, Helv. Chim. Acta, 45 (1962) 506.
[24] E. Gimzewski and S.H. Hawkins, Thermochim. Acta, 99 (1986) 379.
[25] D. Bourgeois, P. Zecchini and C. Devin, C.R. Acad. Sci. Paris, Ser. C, 278 (1974) 53.
[26] S. Gordon and C. Campbell, Anal. Chem., 27 (1955) 1102.
[27] O.A. Momot and M.T. Saibova, Uzb. Khim. Zh., 2 (1976) 11.
[28] C. Ettarh and A.K. Galwey, to be published.
[29] M. Doumeng, Rev. Chim. Miner., 7 (1970) 897.
[30] S.B. Warrington, PhD Thesis, Leeds Polytechnic, 1983.
[31] C. Ettarh and A.K. Galwey, Thermochim. Acta, 261 (1995) 125.
[32] N.J. Carr and A.K. Galwey, Proc. R. Soc. London, Ser. A, 404 (1986) 101.
[33] A.K. Galwey and G.M. Laverty, Thermochim. Acta, 138 (1989) 115.
[34] W. Leithe, The analysis of air pollutants, Ann Arbor Science Publishing, 1971, p. 182.
[35] K.H. Stern, J. Phys. Chem. Ref. Data, 1 (1972) 747.
[36] C.C. Addison and J.M. Coldrey, J. Chem. Soc., (1961) 468.
[37] B.D. Bond and P.W.M. Jacobs, J. Chem. Soc. A, (1966) 1265.
[38] A.K. Galwey and G.M. Laverty, Proc. R. Soc. London, Ser. A, 440 (1993) 77.
[39] M.E. Brown, D. Dollimore and A.K. Galwey, Comprehensive chemical kinetics, Vol. 22, Elsevier, Amsterdam, 1980.
[40] P.I. Protsenko and N.A. Brykova, Russ. J. Inorg. Chem., 8 (1963) 1130.
[41] P.I. Protsenko and E.A. Bordyushkova, Russ. J. Phys. Chem., 39 (1965) 1049.